Technological University Dublin

ARROW@TU Dublin

Conference papers

School of Civil and Structural Engineering

2012

The Response of a Footbridge to Pedestrians Carrying Additional Mass

Darragh O'Sullivan
Technological University Dublin

Colin Caprani
Technological University Dublin, colin.caprani@tudublin.ie

Joe Keogh
Technological University Dublin

Follow this and additional works at: https://arrow.tudublin.ie/engschcivcon

Part of the Structural Engineering Commons

Recommended Citation

The Response of a Footbridge to Pedestrians Carrying Additional Mass

D. O'Sullivan, C.C. Caprani, & J. Keogh
Department of Civil Engineering & Structural Engineering, Dublin Institute of Technology, Ireland
email: darragh.osullivan@ocsc.co.uk, colin.caprani@dit.ie, joe.keogh1@dit.ie

ABSTRACT: Footbridges with low natural frequency are susceptible to excessive vibration serviceability problems if the pedestrian pacing frequency matches the bridge natural frequency. Much research has been done into describing the response of a footbridge to single pedestrian loading. However, many pedestrians carry additional mass such as shopping bags and backpacks, and this has generally not been accounted for in previous research. This work examines this problem using an experimental bridge excited with many single pedestrian events, both with and without additional mass. The vertical acceleration response is measured and compared to moving force, moving mass, and moving spring-mass-damper models. The influence of the additional mass on the results is assessed. It is shown that current theoretical models do not provide an accurate description of the walking forces applied by a pedestrian traversing an excessively vibrating structure. When a pedestrian carries additional mass the response of the footbridge increases however the theoretical models overestimate this increase.

KEY WORDS: Pedestrian; Bridge; Vibration; Mass; Modal; Finite element; Experiment.

1 INTRODUCTION

1.1 Background

With improved design techniques, modern footbridges have become increasingly slender and often have a low vertical natural frequency. Pedestrian pacing occurs at a frequency of about 2 Hz and if this is similar to the footbridge natural frequency, vibration problems can result. The mass of the pedestrian is also an important component of the excitation imparted to the bridge. Further, many pedestrians also carry additional mass, especially in a city environment (such as commuters or shoppers, for example).

In the assessment of footbridge vibrations, the mass used in pedestrian excitation models is commonly understood to be the body mass of the pedestrian. Additional carried mass has not been generally included in the literature [1]. It has been noted [2] that a pedestrian carrying a loaded backpack will adjust their gait to reduce the energy cost of walking and make it more comfortable. The response of a lively footbridge to a pedestrian carrying mass is examined in this paper.

1.2 Approach of this work

This work examines the influence of additional mass on footbridge excitation using physical testing and numerical models. A timber footbridge with low natural frequency is constructed and experimental modal analysis is carried out to determine its dynamic properties. A range of pedestrian loading scenarios are measured. The midspan acceleration response under different pedestrians, both with and without mass, is measured.

The numerical models typically employed to estimate pedestrian excitation are a moving force, moving mass, and a moving spring mass damper model. These models are calibrated to the test conditions and used to predict the measured responses.

1.3 Bridge structure test specimen

A timber footbridge deck is used for the physical testing, as shown in Figure 1. It is designed to have a vertical fundamental natural frequency within a range which is sensitive to pedestrian-induced vibrations. The bridge is simply-supported, 8 m long, and 0.7 m wide. It has a mass of 14.14 kg/m and a flexural stiffness of 422 kNm^2. Transverse bridging pieces are used at 1 m centres to ensure load sharing across the cross-section. The plywood skin is glued to the joists and bridge pieces to ensure full composite action.

(a) experimental set up;
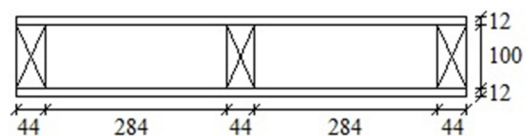
(b) cross-section through bridge deck;

Figure 1. Laboratory testing arrangement.

2 EXPERIMENTAL MODAL ANALYSIS

2.1 Overview of testing

An experimental modal analysis (EMA) is performed on the bridge structure to determine its natural frequencies and their associated damping ratios and mode shapes. The EMA involves simultaneously measuring an input force, $f(t)$, and the resulting output response, $x(t)$. The input force is applied using an instrumented impact hammer. This excitation method is chosen in order to overcome the effects of mass loading which is a critical consideration in the testing of lightweight structures [3].

This paper examines the mid-span response of the model footbridge. As a result, the odd-numbered modes of vibration are of most interest. However, an accelerometer is mounted at quarter span to identify the second mode of vibration also. The impact application and the response measurement are located centrally in the cross-section so that torsional modes are not excited insofar as is possible.

The bridge structure was impacted at three locations along the span; the mid-span and the two quarter-spans (Figure 2) and the resulting acceleration response measured. This results in a time-domain description of the behaviour of the structure. However the frequency-domain behaviour provides a more convenient description from which modal parameters may be extracted. Data is transformed between the time and frequency domain using the Fast Fourier Transform (FFT).
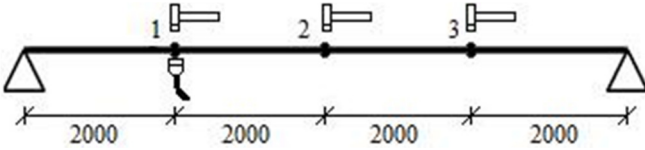

Figure 2. Location of accelerometers and impacts.

A sample period of 25 seconds is measured to allow the vibrations to decay. However, as the structure is very lightly damped, the transient response does not always decay to zero within the sampling period. To minimise the effects of leakage in the transformed data a window (or weighting function) is applied to the measured data. For impact excitation a force window is applied to the input force and an exponential window to the output response [4], [5].

2.2 Estimation of Frequency Response Function

The transducers used to measure the input and output inevitably contain unwanted noise and so averaging is required to minimize its effect on the measurements. The power spectrum of the recorded signal is used for averaging. The Frequency Response Functions (FRFs), $H(\omega)$, for impact testing have been estimated in terms of the cross- and auto-power spectra by Dossing [4] and Ramsey [6] using:

$$H(\omega) = \frac{G_{FX}(\omega)}{G_{XX}(\omega)} \qquad (1)$$

where $G_{FX}(\omega)$ is the cross spectral density between the input $f(t)$ and the output $x(t)$, and is given by:

$$G_{FX}(\omega) = F(\omega)X^*(\omega) \qquad (2)$$

$G_{XX}(\omega)$ is the auto power spectral density of the output $x(t)$:

$$G_{XX}(\omega) = X(\omega)X^*(\omega) \qquad (3)$$

In the above, $F(\omega)$ is the Fourier spectrum of the input $f(t)$, $X(\omega)$ is the Fourier spectrum of the output, and a superscript asterisk denotes the complex conjugate. Equation (1) then yields a complex-valued function of frequency from which the magnitude and phase of the response is calculated [5].

The coherence, $\gamma^2(\omega)$, is a measure of the noise in the system and is defined as [4]:

$$\gamma^2(\omega) = \frac{|G_{FX}(\omega)|^2}{G_{FF}(\omega).G_{XX}(\omega)} \qquad (4)$$

where $0 \leq \gamma^2(\omega) \leq 1$ and $G_{FF}(\omega)$ is the auto power spectral density of the input $f(t)$ and is given by:

$$G_{FF}(\omega) = F(\omega)F^*(\omega) \qquad (5)$$

Ramsey [6] described the coherence in a system as a measure of the 'causality', that is the proportion of the measured response that is caused totally by the measured input. A coherence of 1 implies that there is no noise in the measurements (and so they are 'perfect') whereas a coherence of 0 implies the measurement is pure noise. Of course, in practice perfect measurements are not possible and so coherence will typically be under unity. According to Dossing [4] the coherence will be less than 1 if the location and direction in which the impact is applied is 'scattered', meaning that if the impact is not in the same location and direction each time some variations in results may be expected. The coherence is also expected to be less than 1 where there is an anti-resonance (i.e. where the signal-to-noise is ratio is poor) or the impact point is close to a node point for a particular mode of vibration.

2.3 FRF of unloaded bridge

Using the procedure described, the estimates for the FRF and coherence for each excitation point are determined. The averaged results are shown in Figure 3. Resonant points can be identified by a peak in the FRF magnitude or a value of +/- 90° for the phase. The coherence for each point is low at the lower frequencies for each of the excitation points since the accelerometers have difficulty in recording low frequency signals. The response of the bridge to low frequency excitation is very small. Therefore the signal recorded by the accelerometers at low frequencies is small in comparison to the noise and so a low coherence value is expected. The magnitude of the response at location 2 (mid-span) (shown in Figure 3(d)) is small in comparison to the other three peaks. This is because point 2 is a node point for the second mode. Each of the excitation points is a node point for the fourth mode and so its response is not distinguishable.

The recorded resonant peaks are widely spaced and so locally the FRF is dominated by a single mode. Therefore each peak in the FRF plot can be approximately analysed as the frequency response of a single-degree-of-freedom system. Hence, the modal parameters for the structure are extracted from the FRF magnitude plot of Figure 3(a) and shown in Table 1. Further, the mode shapes can be found from the FRF magnitude and phase plots and are shown in Figure 4.
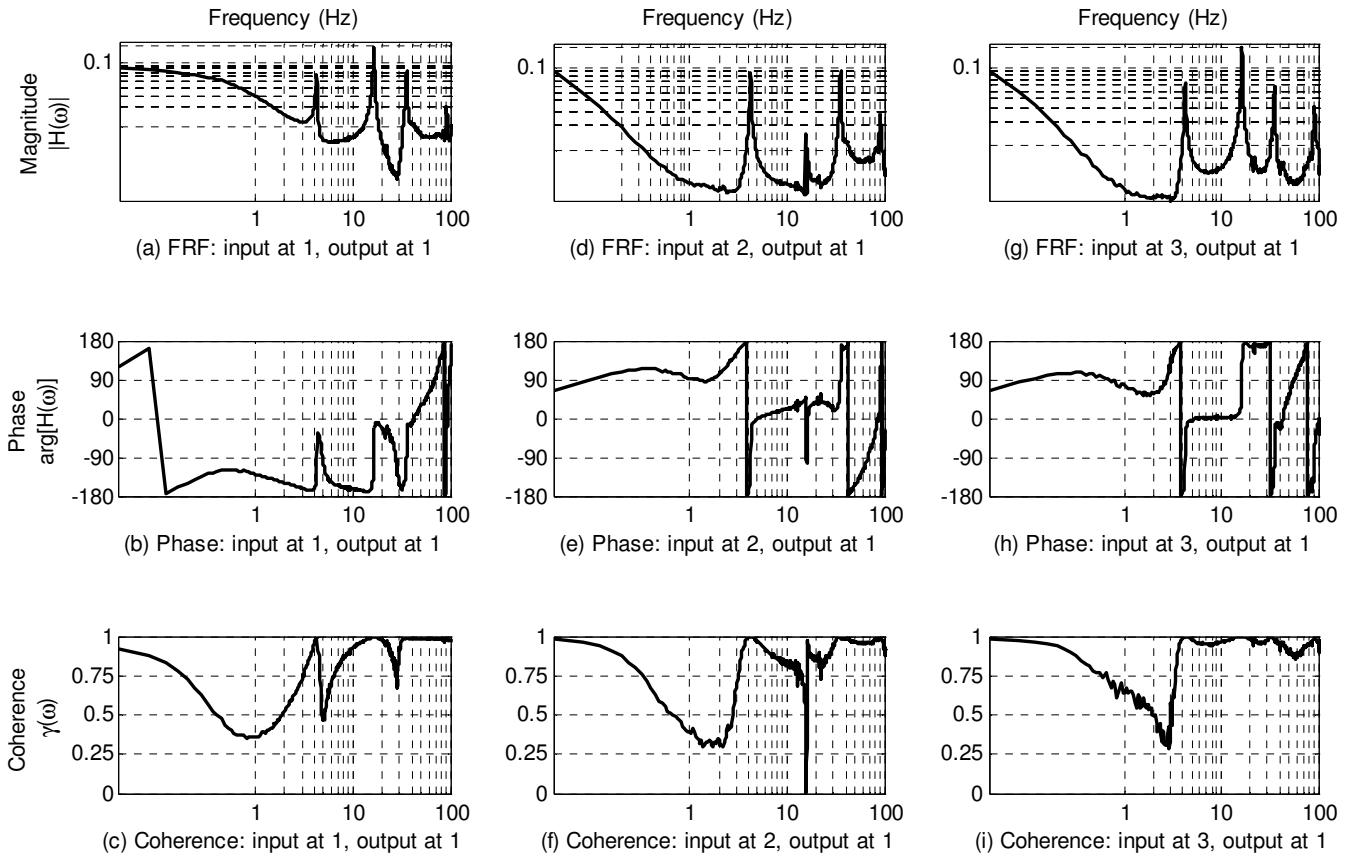
Figure 3. Results of experimental modal analysis (refer to Figure 2 for location numbering).

(a) FRF: input at 1, output at 1
(d) FRF: input at 2, output at 1
(g) FRF: input at 3, output at 1
(b) Phase: input at 1, output at 1
(e) Phase: input at 2, output at 1
(h) Phase: input at 3, output at 1
(c) Coherence: input at 1, output at 1
(f) Coherence: input at 2, output at 1
(i) Coherence: input at 3, output at 1

Table 1. Dynamic properties of the test structure.

Mode	Natural Frequency (Hz)	Magnitude $|H(\omega)|$	Phase $\angle[H(\omega)]$	Damping Ratio
1	4.24	0.0647	-90°	0.0133
2	16.32	0.17260	-90°	0.0092
3	35.64	0.07208	-90°	0.0105
4	n/a	n/a	n/a	n/a
5	91.6	0.01971	-90°	0.0128

The number of mode shapes that can be measured is a function of the number of excitation points on the bridge when a roving output test is used in EMA. In this test set up three impact points were specified and so three mode shapes are determined from the FRF plots. The magnitude of the mode shape is determined from the magnitude of the FRF and the direction from the phase.
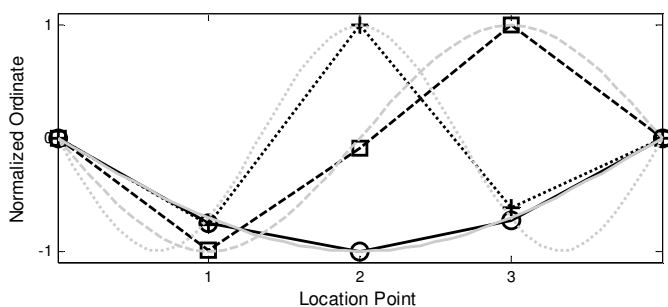

Figure 4. Normalised mode shapes:
Measured – Mode 1 (—⊖—); Mode 2 (—⊟—); Mode 3(┅+┅);
Theoretical – Mode 1 (———); Mode 2 (– – –); Mode 3(┄┄┄).

2.4 Experimental modal analysis with added mass

Due to the low mass of the bridge, the ratio of pedestrian mass to the mass of the test structure is quite large (e.g. 0.71 for an 80 kg pedestrian). Therefore the presence of the pedestrian on the bridge will affect the modal parameters and so further investigations are carried out on these variations. In particular, the variation of the modal parameters as the pedestrian traverses the bridge is of interest. However, this form of EMA is beyond the scope of the present research.

The modal parameters of the structure are determined for two mass scenarios: (a) an 80 kg pedestrian; and (b) an 80 kg inert mass. Both masses are located at mid-span. The driving-point FRF for point 1 (quarter-span) with mass at mid-span is found for both scenarios and the results shown in Figure 5.
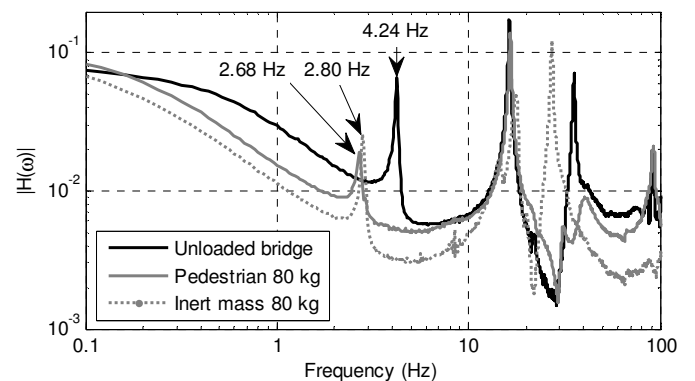

Figure 5. Frequency response functions at point 2 for pedestrian and inert 80 kg masses at mid-span.

By comparison with the unloaded bridge, it can be seen from Figure 5 that the natural frequencies are reduced by the presence of the additional mass as might be expected. Interestingly, there is an additional mode (possibly torsional) with natural frequency at 14.56 Hz for the inert mass.

Using the single-mode approximation described previously, the damping is assessed for each scenario and the results given in Table 2 (along with those for the unloaded bridge from Table 1 for reference). A slight increase in damping is noted for the inert mass. However, under the pedestrian loading, a significant increase in damping of the first mode is evident. This agrees with the findings of Ellis and Ji [7] who suggested the use of a spring-mass-damper model in theoretical analyses to represent human-structure interaction.

Table 2. Damping ratios for bridge loaded with pedestrian and inert 80 kg masses at mid-span.

Mode	Unloaded bridge	Pedestrian mass 80 kg	Inert mass 80 kg
1	0.0133	0.0320	0.0162
2	0.0092	0.0112	0.0301
3	0.0105	*	0.0097
4	n/a	n/a	n/a
5	0.0128	0.0194	**

* Very heavily damped
** No frequency response function peak

3 THEORETICAL MODELLING

3.1 Pedestrian vertical load model

A typical vertical pedestrian force is shown in Figure 6. It is represented by the first harmonic of its Fourier series [8], [9], shown in Figure 6, and given as follows:

$$P(t) = m_P g \left[1 + r \sin\left(2\pi f_p t\right) \right] \qquad (6)$$

In which, m_P is the pedestrian mass, g is the acceleration due to gravity, f_p is the pacing frequency, and r is the dimensionless dynamic force component from Fanning et al [10], given by:
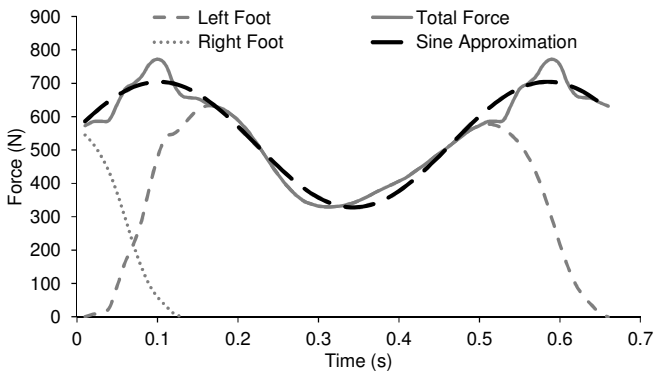
$$r = 0.25 f_p - 0.1 \qquad (7)$$

Figure 6. Typical vertical ground reaction force and approximated model force.

3.2 Pedestrian-bridge systems models

The pedestrian-bridge system models used are shown in Figure 7. They increase in complexity from the moving force model to the rarely-used spring-mass-damper (SMD) model. The moving force model has been commonly used in analysing the pedestrian loading on footbridges [1]. The moving mass model has been used by a few authors, whilst the SMD model is rarely used [11].

The moving force model (Figure 7(a)) does not account for any shift in modal properties due to the presence of the pedestrian, as are internal effects due to the pedestrian mass. These deficiencies are overcome with the moving mass model (Figure 7 (b)) which potentially accounts for both changes in modal properties and inertia of the pedestrian mass. However, the moving mass model assumes equal deflection of the centre of mass of the pedestrian and the bridge surface. This is evidently not correct, as is evident from human location studies [12]. The SMD model of Figure 7(c) accounts for the difference in deflection between the bridge surface and the pedestrian centre of mass by linking the two through a Kelvin-Voight material model representing the human body.
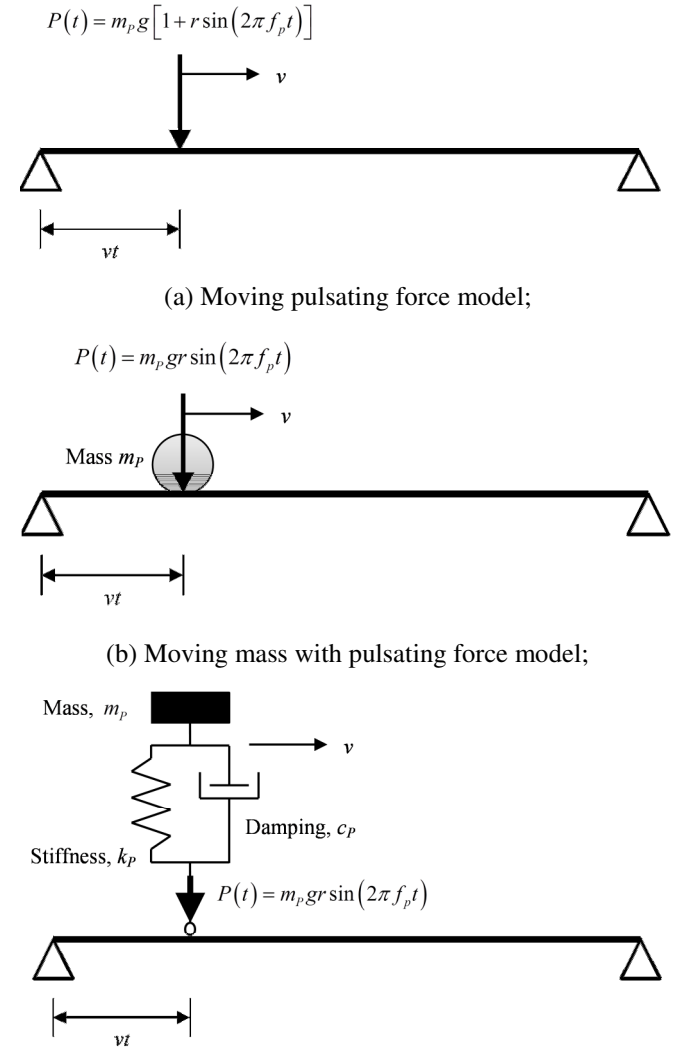
(a) Moving pulsating force model;

(b) Moving mass with pulsating force model;

(c) Moving spring-mass-damper with pulsating force model;

Figure 7. Pedestrian-bridge system models.

3.3 Modal superposition models

Modal superposition can be used to solve for the bridge response for each of the three models of Figure 7. However

the modal superposition method cannot account for any changes in modal properties due to the presence of the pedestrian on the bridge. This may be important when the ratio of pedestrian to bridge mass is significant.

The solution for each of the N modes is found through summation of the equivalent generalized coordinates, q, single-degree-of-freedom model solutions. In this work 10 modes have been used to establish the response. For the moving force (MF) model these are given by [13]:

$$\ddot{q}_j + 2\xi_j\omega_j\dot{q}_j + \omega_j^2 q_j = \frac{m_P g}{M_j}\left[1 + r\sin\left(2\pi f_p t\right)\right]\phi_j\left(vt\right) \quad (8)$$

In which M_j, ξ_j, and ω_j are the modal mass, damping ratio; and circular natural frequency for mode j respectively. The pedestrian position at time t is vt assuming constant velocity v and the mode shape is described by $\phi_j\left(x\right)$. The equation of motion for mode j under the moving mass (MM) model is:

$$\ddot{q}_j + \left\{\frac{m_P}{M_j}\sum_{j=1}^{N}\ddot{q}_j\phi_j^2\left(vt\right)\right\} + 2\xi_j\omega_j\dot{q}_j + \omega_j^2 q_j$$
$$= \frac{m_P g}{M_j}\left[1 + r\sin\left(2\pi f_p t\right)\right]\phi_j\left(vt\right) \quad (9)$$

Finally, the equation of motion for the mode j of the bridge under the SMD model is [13]:

$$\ddot{q}_j + 2\xi_j\omega_j\dot{q}_j + \omega_j^2 q_j + \frac{m_P}{M_j}\ddot{y}\phi_j\left(vt\right)$$
$$= \frac{m_P g}{M_j}\left[1 + r\sin\left(2\pi f_p t\right)\right]\phi_j\left(vt\right) \quad (10)$$

where y is the coordinate describing the motion of the centre of pedestrian mass which has its own equation of motion:

$$m_P\ddot{y} + c_P\dot{y} + k_P y - c_P\dot{q}_j\phi_j\left(vt\right) - k_P q_j\phi_j\left(vt\right) = 0$$
$$j = 1, \ldots., N \quad (11)$$

For the simply supported beam used in this work the modal mass is $mL/2$ where m is the mass per metre of the beam of length L. The mode shape is given by $\phi_j\left(x\right) = \sin j\pi x/L$.

3.4 Finite element models

Finite element models are developed for each of the three pedestrian loading models based on the work of Filho [14], Lin and Trethewey [15], and Majumder and Manohar [16]. For each of these models, the beam is discretized into 10 1-dimensional Euler-Bernoulli beam elements and solved using the Newmark β method assuming consistent mass and Rayleigh proportional damping.

The finite element models have the advantage that changes in modal properties are accounted for as the pedestrian traverses the bridge. However, the discretization of the bridge means that the solution is approximate. However, just as the modal superposition is truncated, it is not expected that much error will results from the use of 10 elements.

4 PEDESTRIAN-INDUCED VIBRATION RESULTS

4.1 Sample result

A typical measurement is shown in Figure 68 along with its calibrated finite element (FE) spring-mass damper model. The response of the bridge is described by a 1 second root-mean-square (RMS) mid-span vertical acceleration. The measured RMS accelerations differ most from the FE SMD model results as the pedestrian reaches mid-span and the response is at its greatest. The sharp peaks in the measured response are due to the heel strike phase of the pedestrian's walking force. This is highest when the pedestrian walks 'downhill', towards mid-span, since the heel has further to travel, prior to making contact with the bridge deck, than it does on a level walking surface. Thus, these heel strike peaks are highest before the pedestrian reaches mid-span and are smaller thereafter.
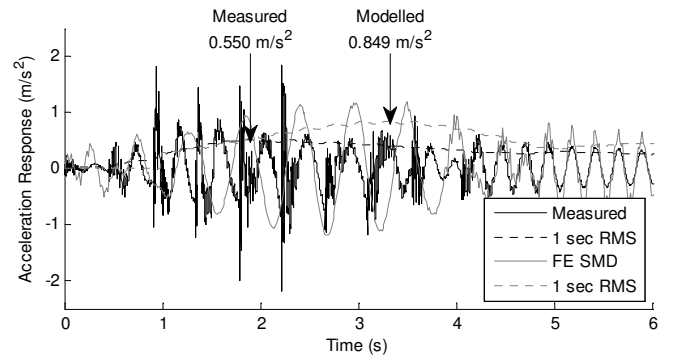

Figure 8. Acceleration response of the bridge to a 64 kg pedestrian with 1.8 Hz pacing frequency.

4.2 Test descriptions

A series of walking tests were conducted and the vertical acceleration response of the footbridge at mid-span was measured. Two male pedestrians traversed the footbridge at a controlled pacing frequency regulated using a metronome. The first pedestrian, Ped_1, with mass 80 kg traversed the bridge with pacing frequencies ranging from 1.8-2.2 Hz in increments of 0.1 Hz, while Ped_2 with mass 64 kg, traversed the bridge with pacing frequencies of 1.8 Hz and 2.0 Hz. A mass of 16 kg was added to Ped_2 to bring his total mass to 80 kg and the tests repeated.

The numerical models previously described are calibrated using the EMA results. The phase of the pedestrian walking force is estimated based on the free-vibration response (e.g. Figure 68). For the SMD models, the spring stiffness and damping is first estimated using population means (see [13]) but then calibrated to give the best-match results.

4.3 Experimental and theoretical results

The complete set of experimental and numerical model results is given in Table 3. The measured results are an average of 2 runs for Ped_1 and 3 runs for Ped_2.

The theoretical accelerations for the 64 kg pedestrian carrying an additional 16 kg are different to that of the 80 kg pedestrian because the test subjects each walked with a different velocity to maintain the required pacing frequency.

Table 3. Measured and numerical 1-second RMS mid-span vertical acceleration responses (m/s^2).

Pedestrian	f_p (Hz)	Measured	FE MF	FE MM	FE SMD	MA MF	MA MM	MA SMD
80 kg	1.8	0.492	0.813	1.209	0.837	0.811	0.815	0.823
	1.9	0.622	0.963	1.567	0.901	0.963	0.965	0.875
	2.0	0.695	1.151	2.192	0.953	1.150	1.153	0.937
	2.1	0.739	1.417	3.292	1.078	1.416	1.421	1.070
	2.2	0.733	1.694	5.300	1.269	1.688	1.702	1.237
64 kg	1.8	0.550	0.650	0.871	0.849	0.649	0.652	0.828
	2.0	0.587	0.917	1.399	1.000	0.918	0.919	0.987
64 + 16 kg	1.8	0.579	0.803	1.182	0.841	0.801	0.805	0.825
	2.0	0.634	1.147	2.142	0.956	1.148	1.149	0.936

From Table 3 it can be seen that each of the theoretical models overestimates the measured acceleration response of the footbridge. Interestingly the least fidelity model, the moving force model, yields the closest match to the measured responses. Further, the theoretical models are more accurate in predicting the response for Ped_2 than for Ped_1. The measured accelerations for Ped_2 carrying additional mass is much lower than the theoretical predictions.

The unknown stiffness and damping parameters of the SMD models are calibrated to give the best match to the measured data. Typically a low value of stiffness gives the best match. As a result, in most cases the SMD model is closest to the measured accelerations.

5 SUMMARY AND CONCLUSIONS

5.1 Summary

The effect of additional mass carried by pedestrians is assessed. Experimental modal analysis is used to determine the properties of the bridge unloaded, loaded with an 80 kg pedestrian, and loaded with an 80 kg inert mass. The masses are found to have a considerable effect on the dynamic properties of the structure. In particular, under the pedestrian, the first-mode damping is found to increase significantly. Acceleration responses are measured for a range of pedestrian loading scenarios, including the carrying of additional mass. It is found that the pedestrian carrying additional mass does not have the same response as a pedestrian of same total mass.

The measured results are compared to predictions from a range of numerical models and are found to be consistently lower than the theoretical predictions. The moving force model is found to give reasonable match to the measurements.

5.2 Conclusions

During the execution of the tests, both pedestrian test subjects remarked on the difficulty in maintaining a controlled pacing frequency on such a lively structure. The 'unpredictability' of the response forced them to alter their gait in order to maintain a controlled pacing frequency while traversing the bridge. The theoretical models do not account for such adaption of stride and this is certainly a source of error. However, the deflection of the test structure is unrealistic for a publicly accessible bridge. It is envisaged that a pedestrian would either slow down, or stop completely if vibrations of such an excessive response occurred thus reducing the vibration of the structure.

REFERENCES

[1] Zivanovic, S., Pavic, A. and Reynolds, P. (2005a), 'Vibration serviceability of footbridges under human-induced excitation: A literature review', *Journal of Sound and Vibration*, 279(1-2), 1-74.

[2] Ren, L., Jones, R.K. and Howard, D. (2004), 'Dynamic analysis of load carriage biomechanics during level walking', *Journal of Biomechanics*, 38, 853-863.

[3] Avitabile, P. (2009), 'Modal Space – In Our Own Little World', Collected articles, available from: http://macl.caeds.eng.uml.edu/umlspace/mspace.html

[4] Dossing, O. (1988), 'Structural testing- Part I, Mechanical Mobility Measurements', Bruel and Kjaer, Naerum, Denmark

[5] Inman, D.J. (2001), *Engineering Vibration*, 2nd Edn., Prentice-Hall

[6] Ramsey, K. A. (1975), 'Effective Measurements for Structural Dynamics Testing, Part I', Sound and Vibration, Vo.. 9, No. 11, 24-35.

[7] Ellis, B. and Ji, T. (1997), 'Human-structure interaction in vertical vibrations', *Structures & Buildings*, ICE, Vol. 122, 1-9.

[8] Rainer, J., Pernica, G. and Allen, D. (1988), 'Dynamic loading and response of footbridges', *Canadian Journal of Civil Engineering*, 15(1), 66-71.

[9] Bachmann, H. and Ammann, W. (1987), *Vibrations in Structures-Induced By Man and Machines*, IABSE, Structural Engineering Document 3, Zurich.

[10] Fanning, P., Archbold, P., Pavic, A and Reynolds, P. (2003), 'Transient response simulation of a composite footbridge to crossing pedestrians', *Recent Developments in Bridge Engineering*, K. Mahmoud, Ed., Swets & Zeitlinger Publishers, Lisse, The Netherlands. ISBN 90 5809 606 8.

[11] Archbold, P. (2008), 'Evaluation of novel interactive load models of crowd loading on footbridges', *Proceedings of 4th Symposium on Bridge and Infrastructure Research in Ireland*, National University of Ireland, Galway, 35-44.

[12] Racic, V., Pavic, A., Brownjohn, J.M.W. (2009), 'Experimental identification and analytical modelling of human walking forces: Literature review', *Journal of Sound and Vibration*, 326(1-2), 1-49.

[13] Caprani, C.C., Keogh, J, Archbold, P. & Fanning, P. (2011) 'Characteristic vertical response of a footbridge due to crowd loading', *Proceedings of the 8th International Conference on Structural Dynamics*, Eurodyn 2011, Leuven, Belgium, July 4th – 6th, 2011.

[14] Filho, F.V. (1978), 'Finite element analysis of structures under moving loads', *Shock and Vibration Digest*, 10(8), 27-35.

[15] Lin, Y.H. and Trethewey, M.W. (1990), 'Finite element analysis of elastic beams subjected to moving dynamic loads', *Journal of Sound and Vibration*, 136(2), 323-342.

[16] Majumder, L. and Manohar, C.S. (2003), 'A time-domain approach for damage detection in beam structures using vibration data with a moving oscillator as an excitation source', *Journal of Sound and Vibration*, 268, 699–716.